Simultaneous Image Quality Improvement and Artefacts Correction in Accelerated MRI

Georgia Kanli[1,2,3], Daniele Perlo[1], Selma Boudissa[1,2], Radovan Jiřík[4], and Olivier Keunen[1,2]

[1]In Vivo Imaging Facility, Luxembourg Institute of Health, Luxembourg. [2]Translational Radiomics Group, Department of Cancer Research, Luxembourg Institute of Health, Luxembourg.

[3]Faculty of Electrical Engineering and Communication, Brno University of Technology, Czech Republic.[4]Institute of Scientific Instruments of the Czech Academy of Sciences, Czech Republic.

P-28

Contact: Georgia.Kanli@lih.lu

Introduction

MR data are acquired in the frequency domain, known as k-space. Acquiring high-quality and high-resolution MR images can be time-consuming, posing a significant challenge when multiple sequences providing complementary contrast information are needed or when the patient is unable to remain in the scanner for an extended period of time. Reducing k-space measurements is a strategy to speed up acquisition, but often leads to reduced quality in reconstructed images. Additionally, in real-world MRI, both under-sampled and full-sampled images are prone to artefacts, and correcting these artefacts is crucial for maintaining diagnostic accuracy. Deep learning methods have been proposed to restore image quality from under-sampled data, while others focused on the correction of artefacts that result from the noise or motion. No approach has however been proposed so far that addresses both acceleration and artefacts correction, limiting the performance of these models when these degradation factors occur simultaneously.

Methods

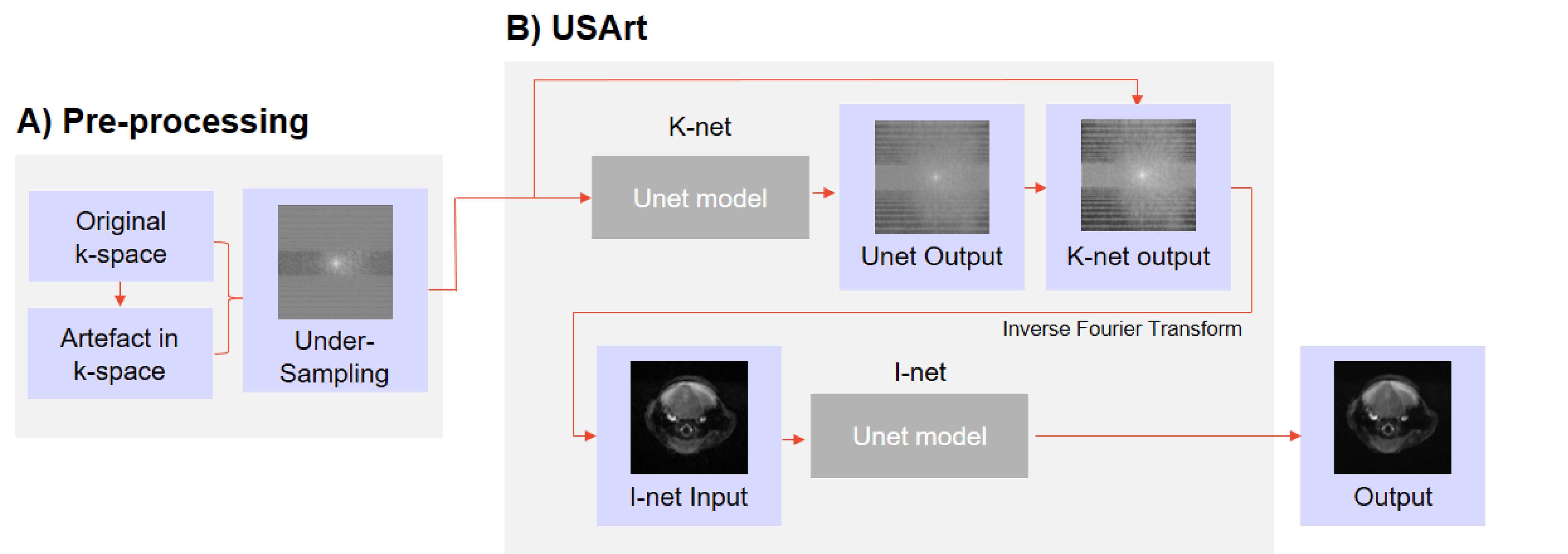

Figure 1 - The preprocessing pipeline and USArt. A) Artifacts and noise are added to full k-space, before under-sampling is performed using specific masks and acceleration factors. This degraded k-space dataset is used as input for the USArt model. B) USArt utilizes two U-Net based components: K-net and I-net. K-net operates in the k-space domain to fill missing lines, and its output is transformed to the image domain via an inverse Fourier Transform. I-net then refines this output, focusing on artifacts correction and image consistency

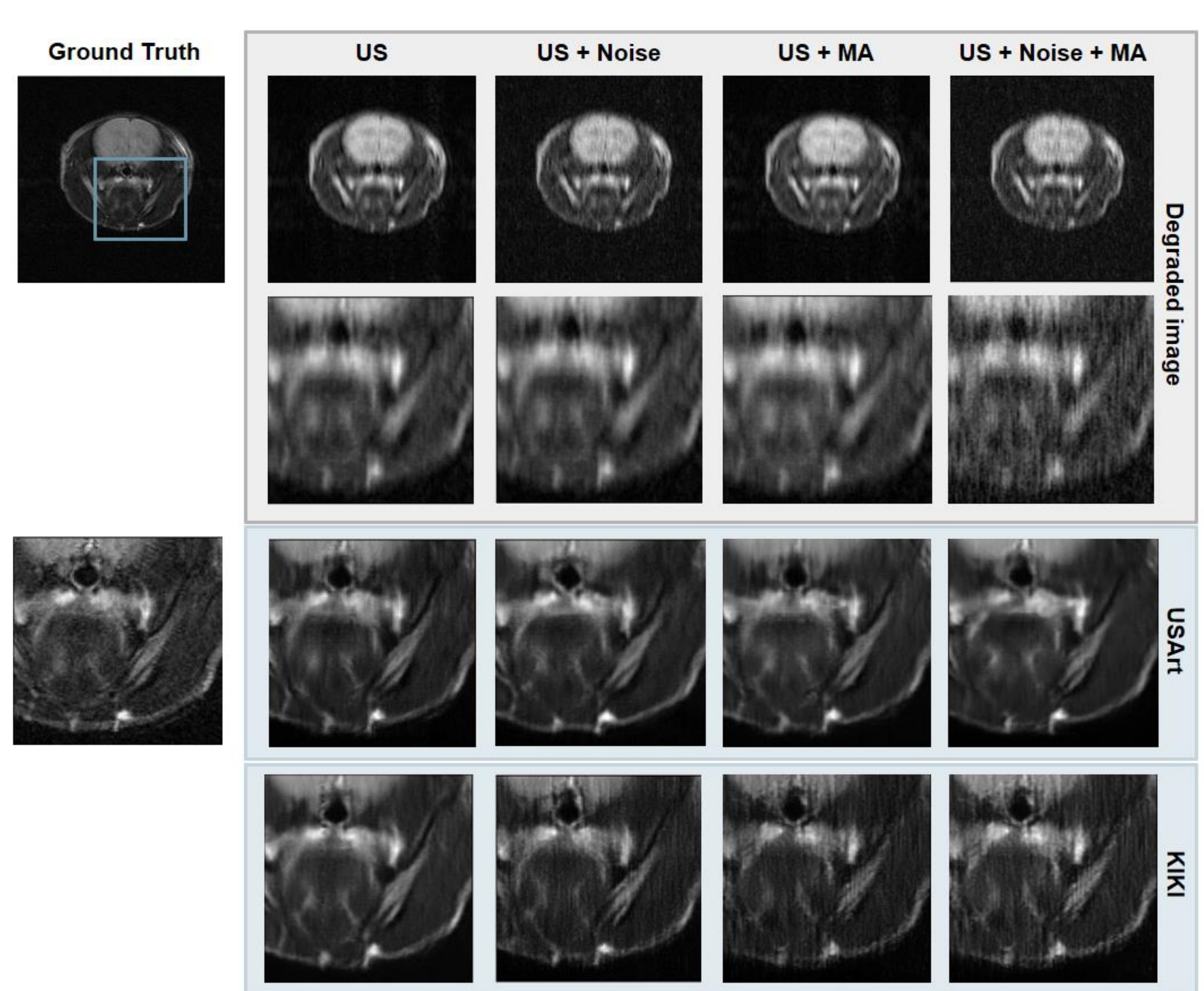

Figure 4 - Illustration of artefacts correction in accelerated images: First column) Original and zoom images (blue frame). Grey box) $5\times$under-sampled full and zoomed images with no artefacts, noise, motion artefact and their combination. Blue box) Corresponding images with quality restored by USArt and KIKI model's. US: Under-sampled, MA: Motion Artifact.

Results

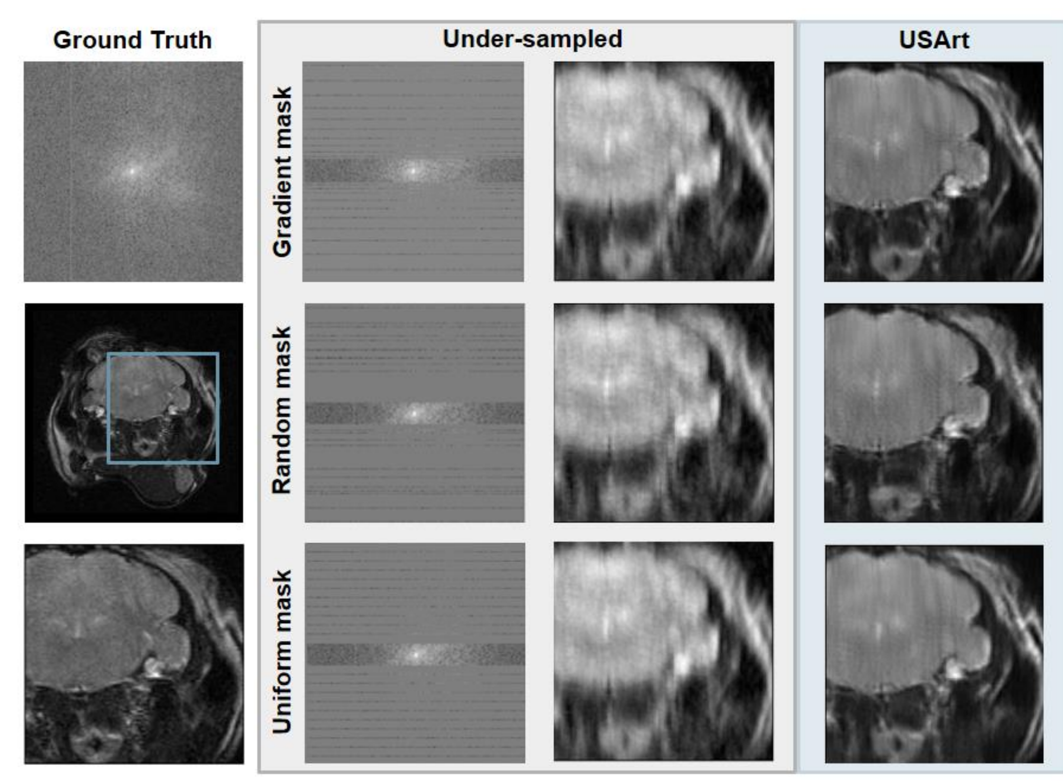

Figure 2 - Under-sampling strategies with acceleration factor 5x: Left column from top to bottom) k-space, reconstructed, and zoom images (blue frame) for the original image. Grey panel) Under-sampled k-space and the zoom corresponding reconstructed images for gradient, corresponding reconstructed images for gradient, random and uniform under-sampling. Blue-light panel) the corresponding USArt's output.

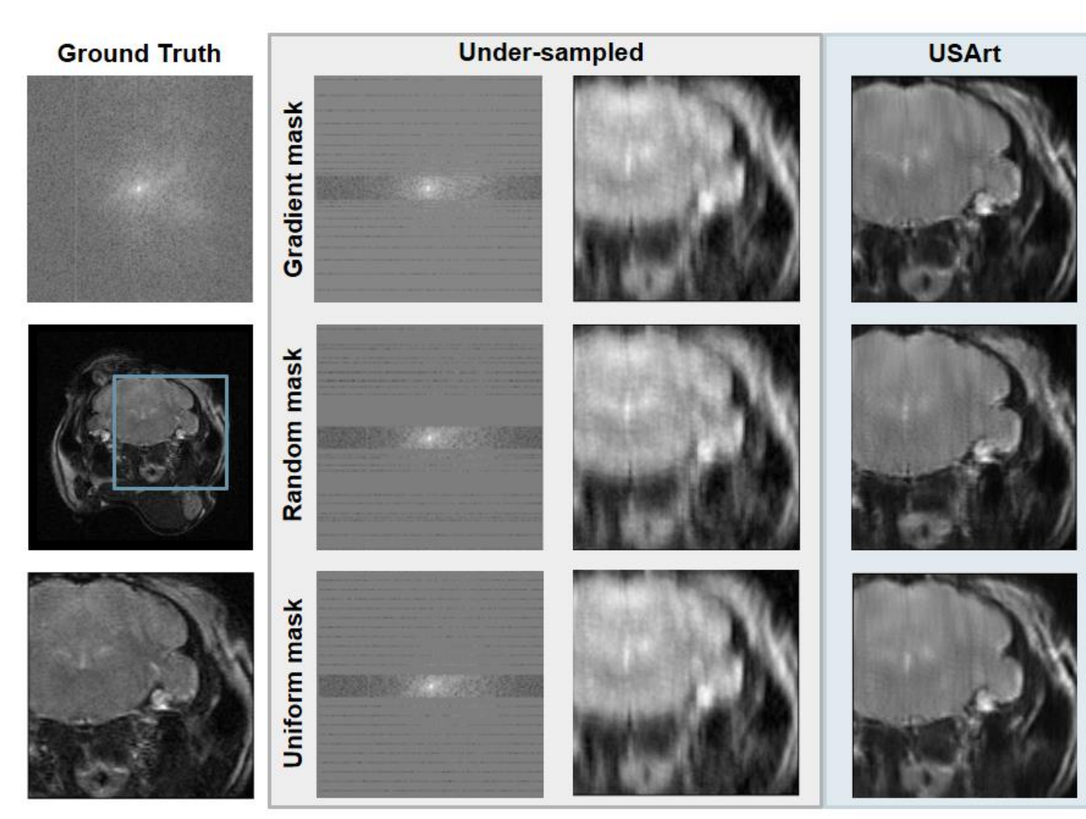

Figure 3 - Different acceleration factors: Left column) from top to bottom: k-space, reconstructed, and zoom images (blue frame) from the original image. Grey panel) Under-sampled k-space and the zoom corresponding reconstructed images for acceleration factors 2x, 5x, and 10x. Blue panel) the corresponding USArt's output.

Acc.	US masks	Artifact	SSIMf	PSNR	SNR	Contrast
	Original	No			15.249 ± 2.170	0.671 ± 0.141
USArt						
5x	Gradient	No	**0.971 ± 0.008**	**77.219 ± 1.436**	**78.976 ± 11.125**	0.710 ± 0.148
5x	Random	No	0.969 ± 0.009	76.586 ± 1.467	78.946 ± 11.868	0.709 ± 0.148
5x	Uniform	No	0.969 ± 0.009	76.541 ± 1.541	75.712 ± 11.558	**0.721 ± 0.152**
2x	Gradient	No	0.979 ± 0.006	78.477 ± 1.457	51.656 ± 4.290	0.708 ± 0.137
5x	Gradient	No	0.971 ± 0.008	77.219 ± 1.436	75.712 ± 11.558	0.710 ± 0.148
10x	Gradient	No	0.962 ± 0.011	74.934 ± 1.798	107.222 ± 16.006	0.746 ± 0.148
5x	Gradient	No	0.971 ± 0.008	**77.219 ± 1.436**	**75.712 ± 11.558**	0.710 ± 0.148
5x	Gradient	Noise	**0.966 ± 0.010**	**76.126 ± 1.747**	**85.638 ± 14.070**	**0.735 ± 0.149**
5x	Gradient	MA	**0.964 ± 0.011**	**75.141 ± 1.816**	55.759 ± 08.380	**0.705 ± 0.143**
5x	Gradient	N+MA	**0.960 ± 0.013**	**74.557 ± 1.607**	**84.251 ± 16.347**	**0.743 ± 0.143**
KIKI [8]						
5x	Gradient	No	**0.971 ± 0.007**	76.496 ± 1.175	**77.125 ± 11.824**	**0.735 ± 0.154**
5x	Gradient	Noise	0.954 ± 0.049	76.091 ± 1.303	44.297 ± 19.010	0.677 ± 0.140
5x	Gradient	MA	0.952 ± 0.013	74.935 ± 1.952	**57.293 ± 20.947**	0.642 ± 0.162
5x	Gradient	N+MA	0.951 ± 0.017	73.179 ± 3.408	40.172 ± 19.683	0.612 ± 0.164

Table 1 - Performance of our proposed model with various under-sampling strategies, acceleration factors, and artefacts. The first three lines compare USArt performance with different under-sampling strategies. The next three lines show USArt performance with different acceleration factors. The next 4 lines show the robustness of USArt to the presence of artefacts. The bottom part of the table provides benchmark values for the reference KIKI~\cite{Eo2018} model using a $5\times$ acceleration factor and gradient under-sampling in the presence of artifacts, showing the superiority of our model in real-world acquisitions.

Conclusion

Acquiring high-quality MR images can be time-consuming. Reducing k-space sampling saves time but typically lowers image quality. The USArt model introduces a novel approach that simultaneously improves image quality and corrects artifacts in accelerated MR imaging. The K-net and I-net sub-models work together to enhance image details, restore contrast, and ensure image consistency. Moreover, the model demonstrates robustness against real-world degradations such as noise and motion artifacts, even when applied to under-sampled data.

Perspectives

Having established confidence in the model's capacity to manage simultaneous under-sampling and artefact correction, future research could explore alternative model architectures such as Vision Transformers. Moreover, our approach is also applicable to accelerating clinical data and other types of trajectories and more advanced protocols, where various types of artefacts may be observed.

References:

1. S. Boudissa, G. Kanli, D. Perlo, T. Jaquet, and O. Keunen, "Addressing artefacts in anatomical mr images: A k-space-based approach," IEEE International Symposiumon Biomedical Imaging, 2024.
2. A. Oudin, V. Baus, V. Barthelemy, C. Fabian, E. Klein, M. Dieterle, M. Wantz, A. C. Hau, C. Dording, A. Bernard, A. Michelucci, Y. A. Yabo, G. Kanli, O. Keunen, R. Bjerkvig, S. P. Niclou, and A. Golebiewska, "Protocol for derivation of organoids and patient-derived orthotopic xenografts from glioma patient tumors," STAR Protocols, vol. 2, 6 2021.
3. T. Eo, Y. Jun, T. Kim, J. Jang, H. J. Lee, and D. Hwang, "Kiki-net: cross-domain convolutional neural networks for reconstructing undersampled magnetic resonance images," Magnetic Resonance in Medicine, vol. 80, pp. 2188–2201, 2018.
4. J. Huang, Y. Fang, Y. Nan, H. Wu, Y. Wu, Z. Gao, Y. Li, Z. Wang, P. Lio, D. Rueckert, Y. C. Eldar, and G. Yang, "Data and physics driven learning models for fast mri – fundamentals and methodologies from cnn, gan to attention and transformers," EEE Signal Processing Magazine, 4 2022.
5. S. Wang, T. Xiao, Q. Liu, and H. Zheng, "Deep learning for fast mr imaging: A review for learning reconstruction from incomplete k-space data," Biomedical Signal Processing and Control, vol. 68, p. 102579, 2021.